Solid-liquid transition in polydisperse Lennard-Jones systems

Sarmistha Sarkar, Rajib Biswas, Mantu Santra, and Biman Bagchi*
Solid State and Structural Chemistry Unit, Indian Institute of Science, Bangalore 560012, India
(Received 11 March 2013; published 5 August 2013)

We study melting of a face-centered crystalline solid consisting of polydisperse Lennard-Jones spheres with Gaussian polydispersity in size. The phase diagram reproduces the existence of a nearly temperature invariant terminal polydispersity ($\delta_t \simeq 0.11$), with no signature of reentrant melting. The absence of reentrant melting can be attributed to the influence of the attractive part of the potential upon melting. We find that at terminal polydispersity the fractional density change approaches zero, which seems to arise from vanishingly small compressibility of the disordered phase. At constant temperature and volume fraction the system undergoes a sharp transition from crystalline solid to the disordered amorphous or fluid state with increasing polydispersity. This has been quantified by second- and third-order rotational invariant bond orientational order, as well as by the average inherent structure energy. The translational order parameter also indicates a similar sharp structural change at $\delta \simeq 0.09$ in case of $T^* = 1.0$, $\phi = 0.58$. The free energy calculation further supports the sharp nature of the transition. The third-order rotationally invariant bond order shows that with increasing polydispersity, the local cluster favors a more icosahedral arrangement and the system loses its local crystalline symmetry. Interestingly, the value of structure factor $S(k)$ of the amorphous phase at $\delta \simeq 0.10$ (just beyond the solid-liquid transition density at $T^* = 1$) becomes 2.75, which is below the value of 2.85 required for freezing given by the empirical Hansen-Verlet rule of crystallization, well known in the theory of freezing.

DOI: 10.1103/PhysRevE.88.022104 PACS number(s): 64.60.−i, 64.70.dj, 05.70.Fh, 05.10.Ln

I. INTRODUCTION

A system that consists of particles with a spread of size, shape, or charge is commonly referred as "polydisperse." There are many materials which are polydisperse in nature, e.g., colloids, polymers, etc. It is now known that polydisperse fluids exhibit many behaviors not observed in monodisperse systems [1–11]. For example, polydisperse systems can exhibit novel phase behavior, such as an intense sensitivity of phase boundaries to the presence of atypical large particles [2], fractionation leading to multiphase coexistence [3–8], as well as remarkable dynamical effects such as an enhanced susceptibility to glass formation [9,10] and the likelihood of multistage relaxation processes [11]. Various earlier studies suggested that beyond an upper limit on the size polydispersity (terminal polydispersity), homogeneous crystallization never takes place [12–16]. This terminal polydispersity and the nature of transition at this point are subjects of great interest [17–20].

About three decades ago Rice and co-workers found an intriguing result in their study of the freezing of hard sphere systems that provides new insight into the random close packed (RCP) state of the hard sphere fluid [21–23]. They also carried out a similar analysis of Lennard-Jones (LJ) fluids [22]. Analysis of the nonlinear integral equations for inhomogeneous density corresponding to freezing to the fcc, by using the bifurcation theory of freezing developed by Kozak *et al*. [24], suggested the existence of a terminal density that can be identified with the RCP state. We shall elaborate on this fascinating result in a bit more detail. In this approach, the transformed order parameter of liquid to solid transition $\psi_{\vec{G}} = \frac{\rho_l}{\rho_s}\phi_{\vec{G}}$ (where $\phi_{\vec{G}}$ is the order parameter that describes freezing and is ultimately related to the Debye-Waller factor, ρ_l and ρ_s are the density of the liquid and solid phases, respectively) was investigated in terms of $\lambda_{\vec{G}}$, where $\lambda_{\vec{G}} = \rho_s \vec{C}_2(\vec{G})$, and $\vec{C}_2(\vec{G})$ is the Fourier transform of the direct pair correlation function $\vec{C}_2(\vec{R}_{12})$, evaluated at the reciprocal lattice vector $\vec{G}$. The bifurcation diagram so obtained exhibited certain interesting features that are independent of interaction potential, determined solely by the lattice type and the dimensionality. The reduced order parameter was found to go continuously to zero at $\lambda_{\vec{G}_\alpha} = 1$, where $\vec{G}_\alpha$ is the first reciprocal lattice vector of fcc, i.e., $(\pm 1, \pm 1, \pm 1)\, 2\pi/a$, where a is the unit cell length. Numerical calculations using the Thiele-Wertheim [25,26] solution for hard spheres of the Percus-Yevick equation provide the following values of the density parameters for liquid to solid transition $\rho_l^* = 1.202$, $\rho_s^* = 1.381$ at $\lambda_{\vec{G}_\alpha} = 1$. Note that beyond $\lambda_{\vec{G}_\alpha} = 1$, no liquid-solid transition can exist. They found the liquid density is close to the random closed pack density of hard spheres obtained by Bernal [27] a long time ago (and verified by many authors since then), and the density of the solid is close to the crystal closed pack density, which is equal to 1.414.

The three-dimensional bifurcation diagram for an fcc lattice predicted a first-order phase transition at lower (than RCP) density, which can be obtained by imposing the equality of thermodynamic potential between the liquid and the solid phases. However, a bifurcation diagram can also be used to address the metastable region in the order parameter space as given by the nonlinear integral equation theory of freezing. Rice and co-workers further speculated that the RCP, where the reduced order parameter $\psi_{\vec{G}_\alpha}$ goes to zero, is the terminal point in the phase diagram where the liquid must transfer to solid [22]. This was considered as the spinodal point of the liquid-solid transition. However, a precise origin of the reason for the RCP state as the terminal transition point is still not clear and remains an intriguing unsolved issue. Clearly transition to crystalline solid can become prohibitively difficult at the RCP state of the liquid where the compressibility

*bbagchi@sscu.iisc.ernet.in

goes to zero and density fluctuations are virtually impossible. Although Rice and co-workers recently exhibited the existence of RCP in binary mixture [28], no study has been carried out for the polydisperse system using the bifurcation diagram.

In one of the previous studies Phan *et al*. [29] reported that large polydispersity favors the formation of a metastable disordered solid. They furthermore found that the crystalline state is usually characterized by an ordered arrangement where larger particles are placed on the corners and smaller particles on faces of the fcc. Thus larger particles are surrounded by twelve smaller particles, whereas smaller particles are surrounded by four larger particles and eight smaller particles. *They made a remarkable observation that the maximum volume fraction of the RCP, i.e.,* $\phi_{\max}^{RCP}$, *is almost independent of polydispersity, whereas maximum volume fraction of fcc i.e.,*$\phi_{\max}^{\mathrm{fcc}}$, *decreases with the increase in polydispersity*. As a result, a crossover between $\phi_{\max}^{\mathrm{fcc}}$ and $\phi_{\max}^{RCP}$ is observed at around 0.12 (see Fig. 10 of Ref. [29]). Thus, beyond this density, no freezing of fluid phase into crystalline solid is predicted to be possible, because the density of the solid becomes less than that of the liquid. This crossover implies that at large polydispersity random packing of hard spheres is more efficient than crystal close packing. Just prior to the crossover, as the polydispersity is increased, the density difference between the random disordered state and the crystalline state (both at the same pressure) is very small, implying that the fractional density change on freezing would also be very small. This is analogous to the freezing of three- and two-dimensional one component plasma to bcc and the hexagonal lattice, respectively [21,23]. In the case of a one component plasma, the fractional density change is zero to preserve electroneutrality of the system. A freezing transition is possible because the compressibility tends to zero, so the energy gain from freezing remains finite and can counter the loss in free energy due to entropy loss upon solidification. In the case of freezing near the RCP state, compressibility tends to zero, making a transition with zero fractional density change thermodynamically possible. The existence of terminal polydispersity and the coincidence of liquid-solid density at the terminal polydispersity with the RCP state bears a resemblance to the analysis of Rice *et al*. [22] for a hard sphere system and also conjectured for the one component Lennard-Jones fluid as the bifurcation diagram for liquid-fcc transition is independent of interaction potential. For Lennard-Jones potential, the density of the RCP state is weakly temperature dependent [29].

Subsequently, several studies of phase behavior of freezing transition of polydisperse hard sphere and repulsive soft sphere fluids have been carried out [5,6,8,30,31]. A significant conclusion from all of these studies is the microscopic fractionation, in which case local polydispersity can be different among the coexisting phases. In polydisperse hard sphere systems, another fascinating observation is the reentrant melting [9,32,33] scenario, which has been observed for hard spheres at large polydispersity and large volume fraction. In those limits, (where pressure is also high) the disordered state is more stable. Therefore the crystalline solid state is bounded by $\phi < \phi_S$ and $\delta < \delta_t$. The reentrant melting has also been observed in experiments [34].

Although an analytical study of freezing or melting of polydisperse fluid is challenging, there have been several notable attempts to study both the fluid-fluid and the fluid-solid transition [1,35]. Recently, an elegant application of density functional theory (DFT) theory of freezing of hard sphere fluid by Chaudhuri *et al*. found a terminal polydispersity of 0.048, followed by a reentrant melting at larger density [16]. In fact, a number of studies on hard sphere polydisperse systems showed the existence of terminal polydispersity as well as reentrant melting [9,32,33]. Experimental studies, however, observed a nearly universal value of 0.12 for the terminal polydispersity [29,36]. Simulation studies on hard sphere crystals also predict a possible terminal polydispersity of 0.113 [37], which is close to the value that Bolhuis and Kofke [38] reported for the terminal polydispersity $\delta_t = 0.118$ for the fluid. Simple mean-field model of polydisperse hard spheres suggests the value to be 0.0833 [32]. It is also well known that for binary systems, the Hume-Rothery rule precludes freezing when the radii of the two components differ by more than 15%, beyond which glass becomes the stable phase at high density [39].

While a sharp increase in liquid-solid surface tension with polydispersity can exclude nucleation of a crystalline nucleus [15], it still leaves open the question of the existence of a thermodynamically stable crystalline phase, at a large polydispersity, marked by a global free energy minimum. DFT analysis, on the other hand, suggests that the crystalline minimum either disappears or becomes metastable with respect to the disordered phase beyond a terminal polydispersity. Thus the situation is again a bit like spinodal decomposition. In the DFT analysis, the reduced stability of the crystalline phase arises from the reduced value of the first peak of the static structure factor, $S(k)$. This is then related to the larger disorder in polydisperse fluids than monodisperse fluids and this disorder increases with polydispersity. However, the said DFT analysis, in addition to predicting a lower value of the terminal polydispersity for hard spheres, does not address the issue of the transition properties, like the polydispersity dependence of the volume fraction change across the transition [16]. Temperature dependence of the transition has not been studied theoretically (most of the studies considered only hard spheres) and thus the phase diagram has not been fully elucidated yet.

In this article we present a computer simulation study of melting of the Lennard-Jones polydisperse system. Our study reveals a remarkable result that *the transition polydispersity converges, when volume fraction is varied, to a maximum value of 0.11, termed as terminal polydispersity, at different temperatures*, in agreement with experiments [34]. The transition line does not show any signature of reentrant melting. Additionally, we find that the fractional volume change on melting or freezing *approaches zero* as we increase the polydispersity at constant temperature. The second-order and third-order rotational invariant bond orientational order parameters show a large amplitude jump as the system passes through the transition polydispersity. The third-order bond orientational order explores that at large polydispersity local crystalline symmetry decreases and structure becomes more icosahedral type. We also show by inherent structure analysis [40] that some of the above results can be understood from the increase in the internal energy of the crystalline phase

with polydispersity. In the present study we also find that at the limiting polydispersity the value of the first peak of static structure factor $S(k)$ falls below the 2.85 needed for freezing, as given by the Hansen-Verlet rule of crystallization [41].

II. SIMULATION DETAILS

We study all simulations using standard molecular dynamics (MD) and Monte Carlo (MC) techniques supplemented by a particle swap algorithm. It is well known that standard simulation techniques may not be fully capable of locating the true thermodynamic equilibrium of the system. The particle swap technique alleviates this lacuna to some extent. The system we study consists of 500 particles with periodic boundary conditions having Gaussian distribution of particle diameters σ,

$$P(\sigma) = \frac{1}{\sqrt{2\pi d^2}} \exp\left[-\frac{1}{2}\left(\frac{\sigma - \bar{\sigma}}{d}\right)^2\right]. \quad (1)$$

The dimensionless polydispersity index is defined as $\delta = \frac{d}{\bar{\sigma}}$, where d is standard deviation of the distribution and $\bar{\sigma}$ is the mean diameter. The particles interact with LJ potential having a constant potential depth. The potential for a pair of particles i and j is cut and shifted to zero, at distance $r_c = 2.5\sigma_{ij}$, where $\sigma_{ij} = (\sigma_i + \sigma_j)/2$. We study for different polydispersity indices starting from δ = 0–0.20 with an increment of 0.01. Both MD and MC simulations have been employed in *NVT*, *NPT,* and *NVE* ensembles. The MC simulations are aided with particle swapping, which enables a faster equilibration in the solid phase. Instead of monitoring the density of the polydisperse system in the case of *NVT* and *NVE* ensembles, it is customary to monitor the volume fraction (ϕ) of the systems. The standard conjugate gradient method [42] has been employed to obtain the inherent structures along an MD trajectory. The free energy calculation has been carried out by using umbrella sampling in *NPT* ensembles. In order to check the finite size effects, we carry out MC simulations with larger system size (2048 particles) as well. The overall physical picture does not change upon variation of system size; however, the transition point shifts toward lower polydispersity.

III. RESULTS AND DISCUSSIONS

A. Quenched phase diagram and terminal polydispersity

The presence of polydispersity makes the phase diagram rich and complex, with the possibilities of the presence of terminal polydispersity and reentrant melting. There exist enormous theoretical and computational studies on polydisperse hard sphere fluids in the literature. Polydisperse hard sphere fluids show first-order fluid to solid phase transition with increasing volume fraction. Further increase of volume fraction leads to reentrant melting of the solid. In addition to the reentrant melting, there is another characteristic feature of the hard sphere system: above a threshold value of polydispersity it does not form solid phase under any condition. Contrary to the hard sphere fluid, there are very few studies on systems such as LJ fluids that have attractive interaction potential. Therefore it is interesting to study such model systems to understand the influence of the attractive part of potential on the above-mentioned characteristics.

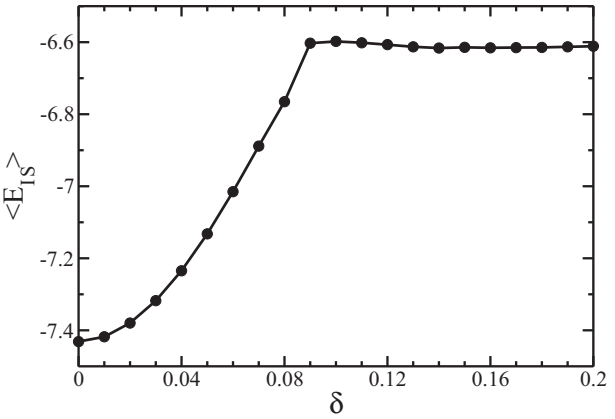

FIG. 1. Variation of average inherent structure energy with respect to polydispersity index at constant volume fraction $\phi = 0.58$ and temperature $T^* = 1.0$. The average IS energy increases almost quadratically with polydispersity until $\delta = 0.09$, when a structural transition takes place and the dependence changes sharply. In the disordered state, average IS energy is nearly independent of polydispersity.

The terminal polydispersity at a different temperature has been calculated in the following fashion. For every polydispersity we carry out *NVT* ensemble simulation for 5×10^4 steps, followed by 5×10^4 steps in the *NVE* ensemble for equilibration and 5×10^5 more steps in the *NVE* ensemble for acquiring results. The single time step size is 2 fs. The standard conjugate gradient method [42] has been employed to obtain the inherent structures along an MD trajectory. We compute the average inherent structure (IS) energy by varying polydispersity. The average inherent structure increases almost quadratically with polydispersity up to a polydispersity index at which structural transition takes place. This polydispersity index is known as "transition polydispersity," beyond which the crystalline solid phase is no longer stable (Fig. 1.).

At a given temperature from average IS energy calculation we obtain the transition polydispersity for a given volume fraction. The transition polydispersity initially increases with increasing ϕ and then becomes invariant at large ϕ [Fig. 2(a)]. Though the transition lines are different for different temperatures, they eventually converge to a value of $\delta_t \sim 0.11$ at large ϕ. There is no liquid-solid transition observed above this polydispersity and it is termed as "terminal polydispersity." Here we should mention that the terminal polydispersity observed in experiments is close to 0.12 in colloidal spheres, which may be modeled as hard spheres [34], and the density functional theoretical prediction of terminal polydispersity of hard spheres is 0.05. The significance of this observation is that for polydispersity higher than δ_t, there is no crystallization and the system inhabits glassy minima. We find that the *terminal polydispersity* is weakly temperature dependent, and for all the temperatures the phase transition ranges between 0.10 and 0.11—the lower limit is obtained at high temperature [see Fig. 2(a)]. The transition line does not show any signature of reentrant melting, as the transition line monotonically increases and gets saturated at higher values of ϕ [Fig. 2(a)].

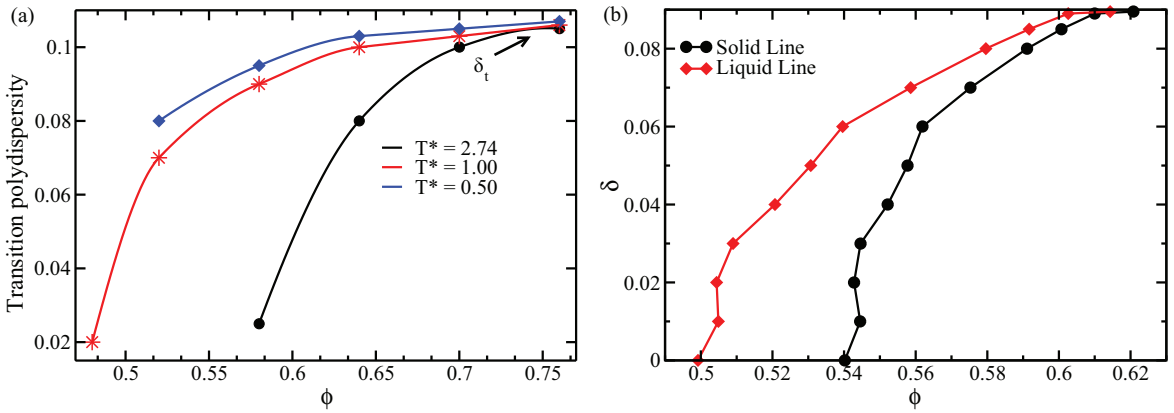

FIG. 2. (Color online) (a) Transition polydispersity obtained from average inherent energy calculation versus volume fraction at three different temperatures $T^* = 0.50$ (blue solid line with filled diamond), 1.0 (red solid line with star), and 2.74 (black solid line with filled circle). Note that the transition polydispersity at different temperatures converges to a maximum value of $\delta_t \sim 0.11$, termed as terminal polydispersity. (b) Phase diagram of the quenched system (i.e., for a given polydispersity only one particle size distribution is studied) in polydispersity-volume fraction plane at $T^* = 1.0$. Note that with increasing polydispersity, the gap between the liquid line and the solid line decreases and at 9% the difference becomes negligibly small (further supported by substantially small compressibility and fractional volume change).

We compute the coexistence line of the solid-liquid transition by varying polydispersity [see Figs. 2(b) and 3] at different temperatures. Figure 2(b) shows the coexistence line at $T^* = 1.0$, whereas Fig. 3 represents the same at four different temperatures $T^* = 0.8$, 0.9, 1.0, and 1.1. Note that with increasing polydispersity the liquid and solid line approach each other, and at 9% polydispersity the density difference of the two phases becomes quite small, less than 1% fractional density change [Fig. 2(b)]. Beyond 9% polydispersity the system does not retain any crystalline solid configuration up to the highest pressures studied. The temperature dependence coexistence line shows that with increasing temperature the fractional density change shifts towards a higher value (Fig. 3). As remarked earlier, we do not observe any reentrant melting scenario.

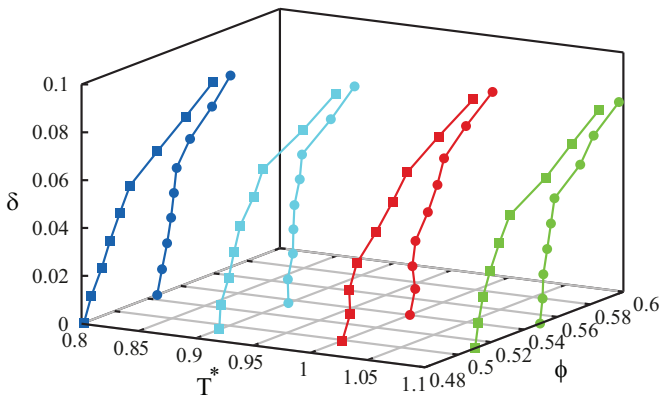

FIG. 3. (Color online) The coexistence lines are shown for four different temperatures: $T^* = 0.8$ in blue, 0.9 in cyan, 1.0 in red, and 1.1 in green. For all the cases the filled square symbol corresponds to the liquid line and the filled circle symbol represents the solid line. With increasing temperature the coexistence volume fraction also increases.

B. Fractional volume change and isothermal compressibility at the transition point

We already discussed earlier that with increasing polydispersity the difference between the density of liquid and solid state at coexistence becomes very small. Here we have computed the fractional volume change at the transition point defined as $(V_L - V_S)/V_S$. Fractional volume change upon melting is computed in the *NPT* system for different polydispersity values at constant reduced temperature $T^* = 1.0$. Figure 4(a) shows that with increasing polydispersity the fractional volume change decreases and eventually becomes very small near the terminal polydispersity. It is further supported by decrease of compressibility (at the spinodal or transition point) with increasing δ, as shown in Fig. 4(b).

Along the transition line the isothermal compressibility (χ) for each polydispersity (δ) has been computed using *NPT* simulation at constant reduced temperature $T^* = 1.0$ and $P^* = 10.0$ Figure 4(b) shows that with increase in polydispersity, the value of the isothermal compressibility (χ) (at the solid-liquid phase transition point) decreases gradually until the polydispersity reaches 0.09, beyond which χ remains almost constant with further increase in polydispersity. This signifies the structural change at $\delta = 0.09$, where the system enters into disordered amorphous or fluid phase. As we all know that isothermal-isobaric compressibility measures the volume fluctuations in the system, consequently, very low compressibility at the transition point provides an explanation for small (∼zero) volume change due to the transition.

C. Quantification of structural change

To quantify the variation in the amplitude of structural change with polydispersity, we compute the local bond order introduced by Steinhardt *et al.* [43], and first apply it to study crystal nucleation by Frenkel and co-workers [44]. Following their definition, a vector $\mathbf{r}_{ij}$ pointing from a given molecule (i) to one of its nearest neighbors (j) is denoted as a "bond." For

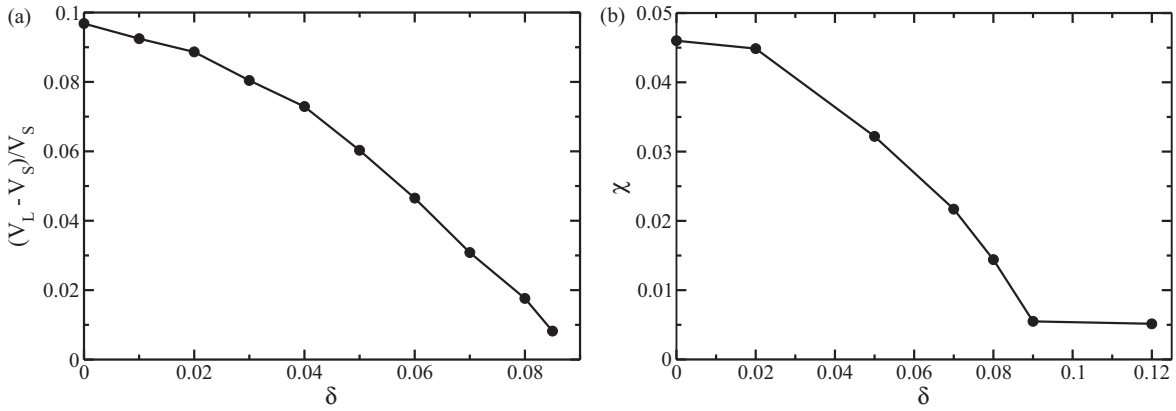

FIG. 4. (a) Fractional volume change against polydispersity index δ. Note that the fractional volume change on the solid-liquid phase transition approaches zero as the polydispersity is increased at constant temperature $T^* = 1.0$. At a polydispersity of 0.09, the fractional volume change is less than 0.01. (b) Variation of compressibility at the transition point with polydispersity index δ. Note that at constant temperature $T^* = 1.0$, as the polydispersity is increased, compressibility decreases and then becomes almost constant from $\delta = 0.09$ onwards.

each bond one determines the quantity

$$Q_{lm}(\mathrm{r}_{ij}) = Y_{lm}[\theta(\mathrm{r}_{ij}),\phi(\mathrm{r}_{ij})], \tag{2}$$

where $Y_{lm}[\theta(\mathrm{r}_{ij}),\phi(\mathrm{r}_{ij})]$ is spherical harmonics and $\theta(\mathrm{r}_{ij})$ and $\phi(\mathrm{r}_{ij})$ are the polar and azimuthal angles of vector r_{ij} with respect to an arbitrary reference frame. The global bond order is obtained by averaging over all bonds in the system,

$$\bar{Q}_{lm} = \frac{1}{N_b}\sum_{\text{bonds}} Q_{lm}(\mathbf{r}_{ij}), \tag{3}$$

where N_b is the number of bonds. To make the order parameters invariant with respect to rotations of the reference frame, the second-order invariants are defined as

$$Q_l = \left[\frac{4\pi}{2l+1}\sum_{m=-l}^{m=l}\bar{Q}_{lm}^2\right]^{1/2} \tag{4}$$

and the third-order invariants are defined as

$$W_l = \sum_{m_1+m_2+m_3=0}\begin{pmatrix} l & l & l \\ m_1 & m_2 & m_3\end{pmatrix}\bar{Q}_{lm_1}\bar{Q}_{lm_2}\bar{Q}_{lm_3}, \tag{5}$$

where the coefficients $(\cdots)$ are the Wigner $3j$ symbols [45]. To measure the symmetry of a cluster in a better way, a normalized quantity is defined as

$$\hat{W}_l = \frac{W_l}{\sum_m (|Q_{lm}|^2)^{\frac{3}{2}}}. \tag{6}$$

In fcc lattice the orientational order is characterized by sixfold symmetry that corresponds to $l = 6$, and, for perfect fcc $Q_6 = 0.5745$ [42,45]. To detect specifically icosahedral order, the preferential choice is W_6 or the normalized quantity $\hat{W}_6$, and for perfect icosahedral arrangement, $\hat{W}_6 = -0.16975$ [43,46]. We have computed Q_6 and $\hat{W}_6$ at $T^* = 1.0$, $\phi = 0.58$ by varying polydispersity of the system [Fig. 5(a)]. Note that in Fig. 5(a) both Q_6 and $\hat{W}_6$ show a sharp structural transition at 9% polydispersity. It is evident from the result that at constant temperature and volume fraction with increasing polydispersity the crystalline order (Q_6) decreases gradually and at 9% polydispersity the crystalline phase disappears completely. It is also clear that with increasing polydispersity, $\hat{W}_6$ becomes more and more negative, which signifies the formation of local icosahedral arrangement. Thus icosahedral arrangement is more tolerant to size asymmetry than crystalline order. The sharp structural transition at 9% polydispersity, indicated by a sharp fall in Q_6 as well as $\hat{W}_6$, confirms the first-order nature of the phase transition.

We also compute the translational order (τ) from the radial distribution function [47,48] as

$$\tau = \frac{1}{s_c}\int_0^{s_c}[g(s)-1]ds, \tag{7}$$

where $s = r\rho^{1/3}$ is the radial distance scaled by the number density, $g(s)$ is the pair correlation function, and s_c is the upper limit of s and set to 3.5. Translational order provides a measure of the local density modulations over a finite number of coordination shells and can be considered as a quantity to characterize the local structure. For a completely uncorrelated system, $g(s) = 1$, and thus τ has a value of zero. On the other hand, the value of τ is relatively large for systems with long-range order. For a perfect fcc crystal it has a value of $\tau^{\text{fcc}}(s_c = 3.5) = 1.7893$. The translational order has been calculated by varying the system polydispersity. The results are shown in Fig. 5(b). The translational order also shows a transition similar to Q_6 and $\hat{W}_6$ at the same polydispersity. Both Figs. 5(a) and 5(b) together confirm a structural transition at 9% polydispersity, at $T^* = 1.0$, and $\phi = 0.58$.

Another unique way of characterization of the structural order that exists in the system is to construct an order map of bond orientational and translation order, shown in Fig. 5(c). It is now well discussed that by increasing the polydispersity the system shows a crystalline solid to fluid phase transition. It is clear from Fig. 5(c) that all crystalline and fluid phases fall onto single lines for each of the respective phases. This means that the two order metrics are strictly correlated and are not independently variable.

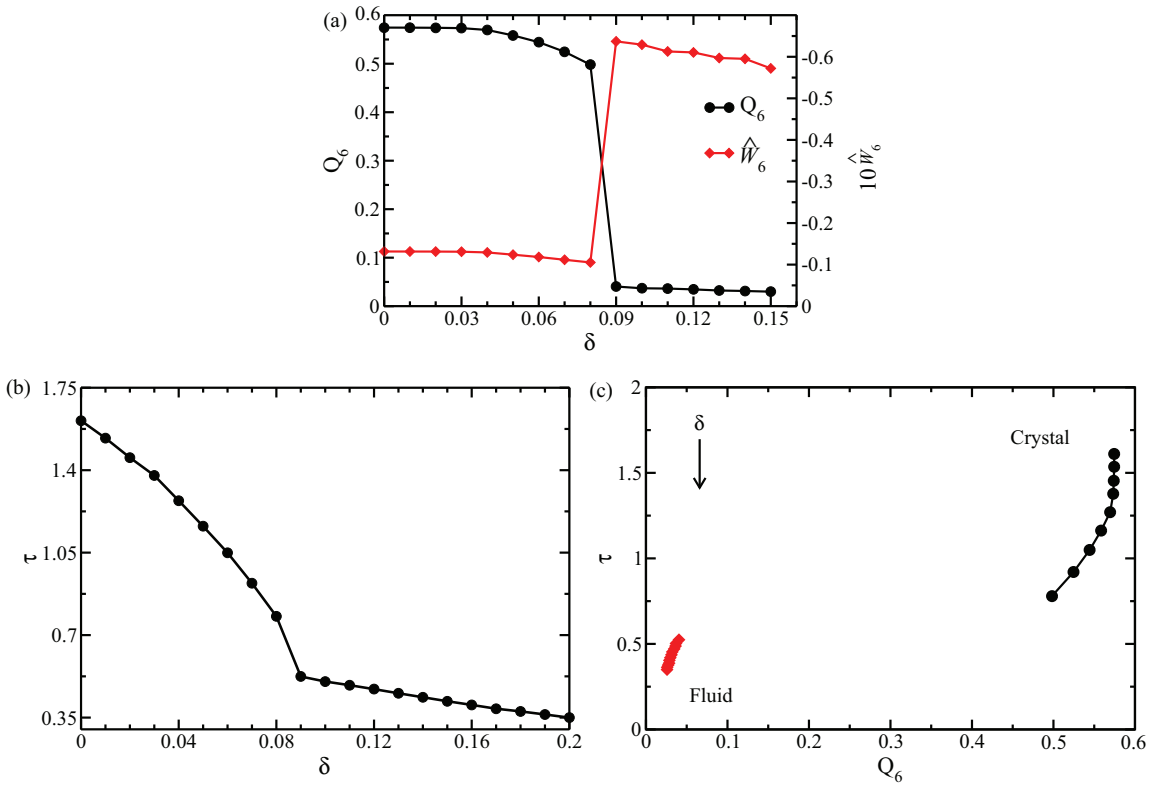

FIG. 5. (Color online) (a) The second-order (Q_6) and third-order (W_6) rotational invariants bond orientational order parameter vs polydispersity. Note with increasing polydispersity the crystalline order (Q_6) decreases and eventually becomes very small, followed by a sharp transition at $\delta = 0.09$, which confirms that homogeneous crystalline phase becomes unstable with increasing polydispersity. On the other hand, the third-order rotational invariants bond order (W_6) becomes more negative, followed by a sharp structural change at same polydispersity. The large negative value (W_6) indicates local clusters that are stabilized by an icosahedral arrangement. (b) Translational order parameter with respect to polydispersity index δ. Note that translational and orientational order together confirm a structural change at 9% polydispersity at temperature $T^* = 1.0$, volume fraction $\phi = 0.58$. (c) Ordering map in τ-Q_6 plane for different δ, at $T^* = 1.0$ and $\phi = 0.58$. It is clear from the order metrics map that two order metrics are highly correlated and are not independently variable.

D. Free energy and existence of metastable amorphous solid

Previously Wales and co-workers have shown that potential energy surfaces can be used to achieve insight into structure, dynamics, and thermodynamics at both a qualitative and a quantitative level [49–51]. We carry out *NPT* simulation and calculate the free energy of the system at different values of polydispersity (δ), at constant temperature $T^* = 1$, and pressure $P^* = 5$, 10, and 15 by using the umbrella sampling technique and considering Q_6 as the order parameter. At a particular pressure, with increasing polydispersity, the crystalline phase becomes gradually less stable and there exists a coexistence polydispersity, (e.g., $\delta \approx 0.07$, for $P^* = 10$), where the free energy of the two states becomes equal [Figs. 6(a)–6(c)]. Upon further increase in δ, the solid becomes less stable, and beyond a particular value of δ, the metastable solid minimum vanishes. Figures 6(a) and 6(b) indicate that the coexistence polydispersity at $P^* = 10$ is $\delta \simeq 0.07$. Upon further increase in δ, the disordered phase becomes more stable and the solid state minimum disappears by $\delta = 0.09$. This is in agreement with the results discussed earlier.

E. Inherent structure energy and polydispersity

Polydispersity makes a first principle study of the melting or freezing transition a bit difficult because analytical solution of pair correlation functions is hard to obtain. Fortunately, one can obtain considerable insight into the melting or freezing process by studying the inherent structures of the liquids and solids and also their energy as a function of the polydispersity. We have discussed earlier (Fig. 1) that average inherent structure energy $\langle E_{IS} \rangle$ increases with polydispersity until a critical value of around $\delta = 0.09$ (at $T^* = 1.0$, $\phi = 0.58$) and then it becomes almost invariant of δ, which indicates a structural change at the polydispersity $\delta = 0.09$. In Fig. 7 we present distribution of IS energy at different polydispersity indices. Note the lack of spread in IS energy distribution until $\delta = 0.085$ (at $T^* = 1.0$, and $\phi = 0.58$). There is a complete change in distribution from polydispersity 0.09 and larger, indicating a structural change and disappearance of homogeneous crystalline solid phase.

F. Discussion

As polydispersity increases, the entropy of the fluid also increases. Thus it is expected that freezing will occur at a higher volume fraction ϕ as the polydispersity index δ increases. In a hard sphere system, this increase in entropy loss on freezing must be counterbalanced by an increase (in absolute magnitude) of the $P\Delta V$ term, where P is the pressure and ΔV is the volume change on freezing. At

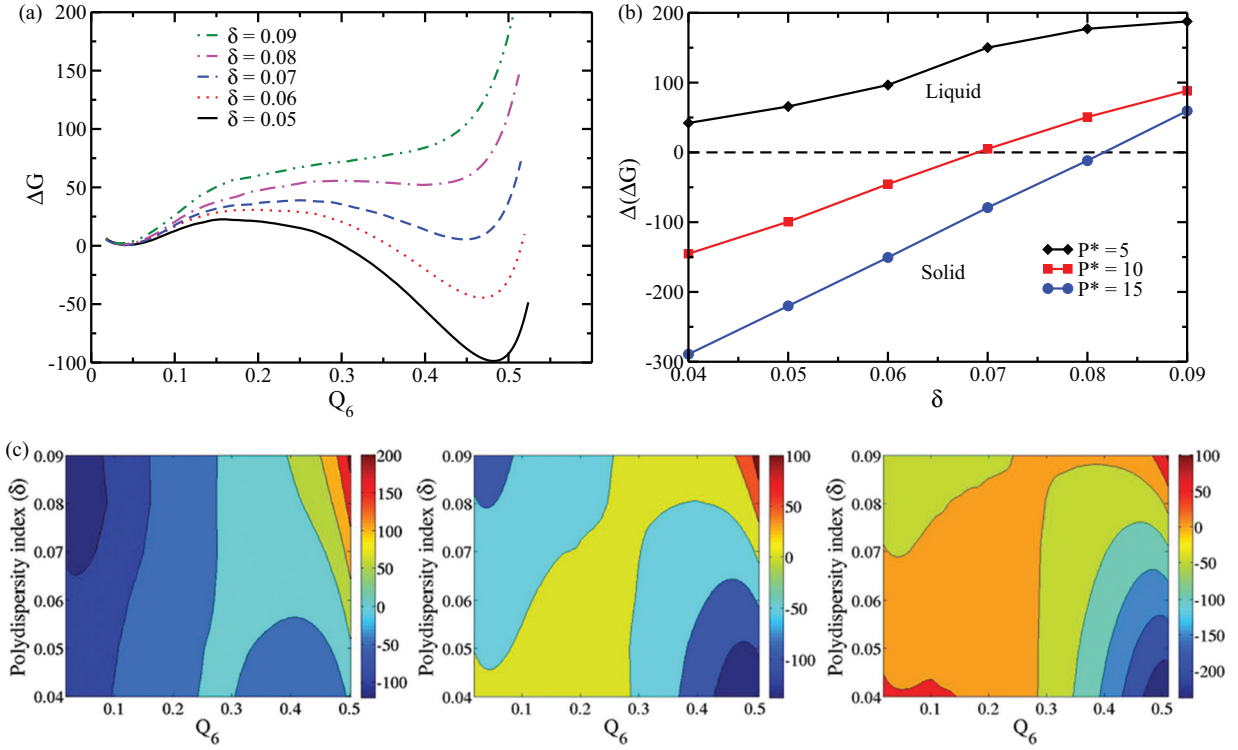

FIG. 6. (Color online) (a) Free energy as a function of Q_6 at temperature $T^* = 1$ and pressure $P^* = 10$ for different polydispersity indices (δ). From figure it is clear that $\delta \sim 0.07$ represents the coexistence point. Note that at $\delta = 0.09$, even the metastable solid phase disappears and the system remains in the liquid phase. (b) The free energy difference of solid phase and liquid phase $[\Delta(\Delta G) = \Delta G_S - \Delta G_L]$ for different polydispersities at temperature $T^* = 1$ and pressure $P^* = 5$ (black, solid line with diamond), 10 (red, solid line with rectangle), and 15 (blue, solid line with circle). From the figure, it is clear that at $P^* = 10$, the system is in coexistence at $\delta \sim 0.07$. (c) Free energy contour as a function of Q_6 at temperature $T^* = 1$ and pressure $P^* = 5$, 10, and 15 (left to right) for different polydispersity (δ). (The contours have been generated by taking $\Delta G_{(Q_6=0.28)} = 0$ as the reference point.) From the figure it is clear that with increase in polydispersity the solid phase becomes more and more unstable and eventually vanishes after the system has approached the terminal polydispersity. The effect of pressure shows that the solid phase is stable at high pressure for $\delta < \delta_t$, and with decrease in pressure the system goes to liquid or amorphous phase, although at $\delta \geqslant \delta_t$ the liquid or amorphous phase becomes the true ground state for any value of pressure.

terminal polydispersity both the $P\Delta V$ term and entropy loss become negligible. For a Lennard-Jones system, an important contribution is made by the change in the internal energy ΔE

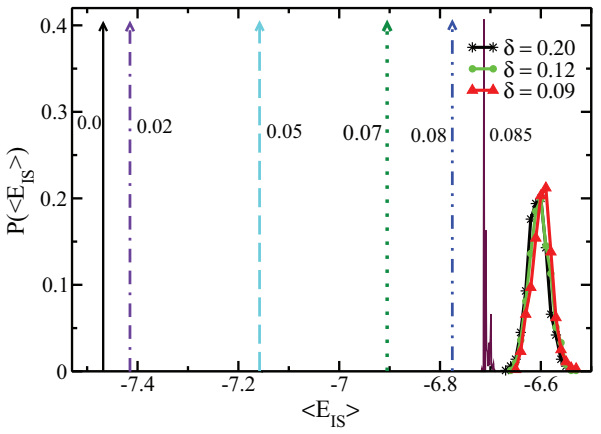

FIG. 7. (Color online) Distribution of IS energy at different polydispersity indices. Note that there is a sharp change in the distribution beyond $\delta = 0.09$ when the distribution assumes the characteristics of a liquid state.

term. Polydispersity dependence of this energy term makes freezing of LJ liquid quite different from that of the hard sphere system, as we report here.

In this manuscript a large number of results pertaining to melting of Lennard-Jones spheres are presented. The first indication of the existence of a possible terminal polydispersity comes from inherent structure analysis, which in a simple way reveals the absence of crystallization at large δ values. The inherent structure analysis also finds a sharp transition between ordered and disordered states. Our analysis shows that the transition line between the liquid and solid ends abruptly at $\delta_t = 0.11$ for all the temperatures studied, beyond which no combination of P and T gives rise to crystallization, that is, the δ_t has a quasiuniversal character. The large ϕ_t (volume fraction at terminal polydispersity) seems to suggest this as an analogy of RCP structure stated by Rice *et al.* and Phan *et al.* [22,29].

Free energy calculation of the order-disorder transition showed the progressive decrease in the stability of ordered state with increase in δ values and for $P^* = 10$ and $T^* = 1.0$. The coexistence of solid and liquid phases is obtained at $\delta = 0.07$ with solid and liquid phase volume fractions, $\phi_s = 0.55$ and $\phi_l = 0.53$, respectively. Free energy calculation

also reveals a spinodal-like behavior when the crystalline state loses even its metastable character and the minimum of solid phase disappears. The value of δ at the "spinodal" point depends on pressure and temperature and forms a locus in the phase plane span by δ, P, and T. Thus the increase in polydispersity acts similarly to be a stress on the system. Therefore the polydispersity-induced solid-liquid transition observed here is similar to the stress-induced mechanical instabilities found in glass. The absence of freezing beyond a terminal polydispersity can also be rationalized by using the integral equation theory of freezing derived from density functional theory, which we discuss elaborately in the Supplemental Material [52].

We find that the compressibility of the liquid state decreases to zero at the pressure where the liquid-solid transition ceases to exist. This happens at the terminal polydispersity. Just prior to the terminal polydispersity, the fractional density change approaches the zero value. In such a situation, the contribution of the $P\Delta V$ term to the free energy change on freezing becomes nontrivial and needs careful consideration. As at every P and T, the $\delta_{\max}(P,T)$ signals the terminal polydispersity beyond which no liquid-solid transition is possible. This is an intriguing result that the fractional volume change approaches zero at every $\delta_{\max}$, which seems to agree with the vanishing compressibility of the system. Such a situation has been observed for three-dimensional and two-dimensional freezing of one component plasma.

The second- and third-order rotational invariant bond orientational orders further support for a structural change at $\delta = 0.09$. The third-order rotational invariant bond orientational further explores that with increasing polydispersity the local arrangement shifts from crystalline to icosahedral type. We thus provide evidence that local icosahedral order suppresses crystalline order in polydisperse Lennard-Jones systems.

Interestingly, our result related to terminal polydispersity can be analyzed using the Hansen-Verlet rule of crystallization. In the present study we find that at the limiting polydispersity, the value of structure factor $S(k)$ of the amorphous phase at $\delta \simeq 0.10$ (just beyond the solid-liquid transition density at temperature $T^* = 1$) attains a value of 2.75 in its first peak, which is below the value of $S(k) \simeq 2.85$ required for freezing given by the well-known Hansen-Verlet rule of crystallization in the field of theory of freezing. This suggests that a polydisperse liquid does not have the required short-range order necessary to transform into a periodic long-range order. The well-known Hansen-Verlet rule provides a nearly universal structural criteria for a dense liquid to crystallize into solid. In its simple form the rule states the crystallization occurs when the first peak of the static structure factor $S(k)$ touches the value 2.85 when temperature T is lowered or density increased. The microscopic explanation of this structural criteria comes from density functional theory that uses the static structural factor of liquid evaluated at the reciprocal lattice vectors (RLVs) of liquid as the response of liquid to periodic density fluctuations. Both for fcc and bcc lattices, a prominent RLV nearly coincident with the wave vector where $S(k)$ has its first (and most prominent) maximum.

All the above results can be rationalized in the following fashion. As δ increases the entropy of the liquid also increases and at a constant volume fraction pressure decreases. Therefore one needs to increase the volume fraction to offset this effect. However, as δ increases, the increase of volume fraction makes efficient packing a difficult process as disorderliness in the system increases, which can even led to fractionation. As shown in Figs. 6(b) and 6(c), increase of pressure makes the solid more stable at low values of polydispersity, but the same ceases to happen when polydispersity increases beyond the terminal value.

IV. CONCLUSIONS

The freezing of polydisperse LJ fluids presents an interesting case because the energy-entropy balance becomes increasingly unfavorable for the solid to exist as a stable phase as the polydispersity increases. The energy of the solid increases due to buildup of strain energy because of the difference in the size of the neighbors, while the entropy of the liquid increases. It is plausible that the crystalline solid may also exist in a large number of minima that involve different degrees of fractionation. While a global minimum of the fractionated crystal can exist, its precise configuration in terms of particle distribution appears to be a bit ill defined. The last statement is meant to imply that there have to be many minima adjacent to the global minimum. So crystallization can happen from an isotropic liquid to any of the anisotropic solids. These two factors lead to the existence of a terminal polydispersity. Note that beyond $\delta \simeq 0.11$, the system remains in the disorder state even at very high pressure and low temperature. In an earlier paper, Rice *et al*. suggested *that the spinodal point of liquid-solid transition of a Lennard-Jones fluid is effectively a random close packing state* and that *no freezing transition is possible beyond this point* [22,28]. It is interesting to find correlation of the present study with this earlier work. This is also in agreement with simulation results of Ref. [29].

Polydisperse systems are good glass formers. Elsewhere we have discussed a fragile to strong liquid crossover as the value of the polydispersity index δ is increased [18,53] at constant volume fraction. This is because the existence of particles of different size interferes with the buildup of dynamical correlations necessary for fragility. Large polydispersity also interferes with buildup of static intermolecular correlations and makes formation of a crystalline state from the liquid phase difficult.

The present study with its focus on inherent structure analysis and free energy calculation compliments earlier studies restricted mostly to repulsive potential. The absence of reentrant melting in the present system may be attributed to the stabilization of solid by the attractive potential. This point deserves further study. It is also shown that at high volume fraction emergence of local icosahedral ordering eventually suppresses crystalline order in large polydispersity.

ACKNOWLEDGMENTS

We thank Prof. C. Dasgupta and Dr. B. Jana for many helpful discussions. This work was supported in parts by Grants from DST and CSIR (India). B.B. thanks DST for support through a J.C. Bose Fellowship. R.B. thanks CSIR for providing support through a Senior Research Fellowship.

[1] P. Sollich, J. Phys.: Condens. Matter **14**, R79 (2002).
[2] N. B. Wilding, P. Sollich, and M. Fasolo, Phys. Rev. Lett. **95**, 155701 (2005).
[3] L. Bellier-Castella, M. Baus, and H. Xu, J. Chem. Phys. **115**, 3381 (2001).
[4] P. Bartlett, J. Chem. Phys. **109**, 10970 (1998).
[5] R. M. L. Evans, Phys. Rev. E **59**, 3192 (1999).
[6] P. Sollich and N. B. Wilding, Phys. Rev. Lett. **104**, 118302 (2010).
[7] R. M. L. Evans, D. J. Fairhurst, and W. C. K. Poon, Phys. Rev. Lett. **81**, 1326 (1998).
[8] M. Fasolo and P. Sollich, Phys. Rev. Lett. **91**, 068301 (2003).
[9] P. N. Pusey, E. Zaccarelli, C. Valeriani, E. Sanz, W. C. K. Poon, and M. E. Cates, Philos. Trans. R. Soc. A **367**, 4993 (2009).
[10] E. Zaccarelli, C. Valeriani, E. Sanz, W. C. K. Poon, M. E. Cates, and P. N. Pusey, Phys. Rev. Lett. **103**, 135704 (2009).
[11] P. B. Warren, Phys. Chem. Chem. Phys. **1**, 2197 (1999).
[12] D. J. Lacks and J. R. Wienhoff, J. Chem. Phys. **111**, 398 (1999).
[13] D. A. Kofke and P. G. Bolhuis, Phys. Rev. E **59**, 618 (1999).
[14] S. R. Williams, I. K. Snook, and W. van Megen, Phys. Rev. E **64**, 021506 (2001).
[15] S. Auer and D. Frenkel, Nature (London) **413**, 711 (2001).
[16] P. Chaudhuri, S. Karmakar, C. Dasgupta, H. R. Krishnamurthy, and A. K. Sood, Phys. Rev. Lett. **95**, 248301 (2005).
[17] J.-P. Hansen and I. R. McDonald, *Theory of Simple Liquids*, 3rd ed. (Academic Press, New York, 2006).
[18] S. E. Abraham, S. M. Bhattacharrya, and B. Bagchi, Phys. Rev. Lett. **100**, 167801 (2008).
[19] A. J. Hopkins and L. V. Woodcock, J. Chem. Soc., Faraday Trans. **86**, 3419 (1990).
[20] K. Maeda, W. Matsuoka, T. Fuse, K. Fukui, and S. Hirota, J. Mol. Liq. **102**, 1 (2003).
[21] B. Bagchi, C. Cerjan, and S. A. Rice, J. Chem. Phys. **79**, 5595 (1983).
[22] B. Bagchi, C. Cerjan, and S. A. Rice, J. Chem. Phys. **79**, 6222 (1983).
[23] B. Bagchi, C. Cerjan, and S. A. Rice, Phys. Rev. B **28**, 6411 (1983).
[24] J. J. Kozak, S. A. Rice, and J. D. Weeks, Physica **54**, 573 (1971).
[25] E. Thiele, J. Chem. Phys. **39**, 474 (1963).
[26] M. S. Wertheim, Phys. Rev. Lett. **10**, 321 (1963).
[27] J. D. Bernal, Nature (London) **183**, 141 (1959).
[28] X. Xu and S. A. Rice, Phys. Rev. E **83**, 021120 (2011).
[29] S.-E. Phan, W. B. Russel, J. Zhu, and P. M. Chaikin, J. Chem. Phys. **108**, 9789 (1998).
[30] N. B. Wilding and P. Sollich, Europhys. Lett. **67**, 219 (2004).
[31] N. B. Wilding and P. Sollich, J. Chem. Phys. **133**, 224102 (2010).
[32] P. Bartlett and P. B. Warren, Phys. Rev. Lett. **82**, 1979 (1999).
[33] M. Tokuyama and Y. Terada, J. Phys. Chem. B **109**, 21357 (2005).
[34] P. N. Pusey and W. van Megen, Nature (London) **320**, 340 (1986).
[35] R. Fantoni, D. Gazzillo, A. Giacometti, and P. Sollich, J. Chem. Phys. **125**, 164504 (2006).
[36] S. M. Underwood, J. R. Taylor, and W. van Megen, Langmuir **10**, 3550 (1994).
[37] E. Dickinson and R. Parker, J. Phys. Lett. **46**, L229 (1985).
[38] P. G. Bolhuis and D. A. Kofke, Phys. Rev. E **54**, 634 (1996).
[39] W. B. Pearson, *A Handbook of Lattice Spacings and Structures of Metals and Alloys* (Pergamon, London, 1958).
[40] D. J. Wales, *Energy Landscapes* (Cambridge University Press, Cambridge, UK, 2003).
[41] J.-P. Hansen and L. Verlet, Phys. Rev. **184**, 151 (1969).
[42] W. Press, B. Flannery, S. Teukolsky, and W. Vetterling, *Numerical Recipes in Fortran 77: The Art of Scientific Computing* (Cambridge University Press, Cambridge, UK, 1992).
[43] P. J. Steinhardt, D. R. Nelson, and M. Ronchetti, Phys. Rev. B **28**, 784 (1983).
[44] S. Auer and D. Frenkel, J. Chem. Phys. **120**, 3015 (2004).
[45] L. D. Landau and L. M. Lifshitz, *Course of Theoretical Physics, Volume III: Quantum Mechanics (Non-Relativistic Theory)* (Butterworth-Heinemann, Oxford, UK, 1981).
[46] Y. Wang, S. Teitel, and C. Dellago, J. Chem. Phys. **122**, 214722 (2005).
[47] J. R. Errington, P. G. Debenedetti, and S. Torquato, J. Chem. Phys. **118**, 2256 (2003).
[48] T. M. Truskett, S. Torquato, and P. G. Debenedetti, Phys. Rev. E **62**, 993 (2000).
[49] J. P. K. Doye and D. J. Wales, J. Chem. Phys. **102**, 9673 (1995).
[50] D. J. Wales and T. V. Bogdan, J. Phys. Chem. B **110**, 20765 (2006).
[51] D. J. Wales and J. P. K. Doye, J. Chem. Phys. **103**, 3061 (1995).
[52] See Supplemental Material at http://link.aps.org/supplemental/10.1103/PhysRevE.88.022104 for an analysis based on the integral equation theory of freezing derived from density functional theory.
[53] S. E. Abraham and B. Bagchi, Phys. Rev. E **78**, 051501 (2008).